Numerical simulation of the effects of InAlSb barrier layers on the InSb mid-infrared photodetectors on a mismatched substrate

Zhao, Zhiqin, Qian, Xu, Wang, Bowen, Jia, Bowen

Zhiqin Zhao, Xu Qian, Bowen Wang, Bowen Jia, "Numerical simulation of the effects of InAlSb barrier layers on the InSb mid-infrared photodetectors on a mismatched substrate," Proc. SPIE 11184, Optoelectronic Devices and Integration VIII, 1118411 (19 November 2019); doi: 10.1117/12.2536915

SPIE.

Event: SPIE/COS Photonics Asia, 2019, Hangzhou, China

Numerical simulation of the effects of InAlSb barrier layers on the InSb mid-infrared photodetectors on a mismatched substrate

Zhiqin Zhao, Xu Qian, Bowen Wang, and Bowen Jia*

College of Information Engineering, Wuhan University of Technology, Wuhan, 430070, China

ABSTRACT

Epitaxial growth of a high-quality InSb layer on a mismatched substrate which provides a path to monolithically integrate InSb-based photonic devices and Si/GaAs-based electronic devices on a single wafer. This work is an attempt to investigate the effects of $In_{0.9}Al_{0.1}Sb$ electron barrier layers on the electrical and optical properties of the InSb photodetectors on a mismatched substrate. The structure of InSb photodetector is p-i-n type where i-layer is the unintentionally n-type doped. A 25 nm $In_{0.9}Al_{0.1}Sb$ layer locates in the i-layer. At 77 K, InAlSb barrier can effectively decrease dark current due to it completely suppresses the generation and recombination current and tunneling current and partially suppresses the diffusion current. The different dark current mechanisms (diffusion, generation and recombination, tunneling) are discussed associated with the bandgap diagrams. For the simulation of photoresponse, the incident light is set to be 5.3 μm. At 77 K, the existence of InAlSb layer doesn't influence the absorption of incident light due to its limited thickness, however, the InAlSb layer separates the i-layer and impedes the transportation of electrons. Therefore, the InAlSb layer decrease the photoresponse of InSb detector and its effects is more remarkable when the diffusion length of hole is around 5 μm or its location is near the surface of the detector. According to the simulation, optimizing the location of the $In_{0.9}Al_{0.1}Sb$ is important to increase the performance of InSb photodetectors on a mismatched substrate.

Keywords: InSb photodetector, Barrier layer, Mid-infrared, Narrow bandgap, Dark current, Photonic integrated circuits, Mismatched substrate, Simulation

*jiabowen@whut.edu.cn

1. INTRODUCTION

In the past two decades, mid-infrared (3-8 μm) region attracted more and more research interest due to its potential applications in the environmental monitoring, biomedicine, thermal imaging, and automatic industry [1]. Moreover, the 3-5 μm MIR light transmits in the atmosphere with very low loss , therefore, it can be used in free-space communication [2]. Due to its 300 K bandgap of 0.17 eV and 77 K bandgap of 0.23 eV, InSb photodetector can cover the whole MIR region and its robust chemical properties and mature fabrication process ensure the high performance and low cost of InSb photodetector [3]. Recently, the commercial InSb PIN photodetector has achieved the 77 K detectivity of 1.6×10^{11} $cmHz^{1/2}/W$ at 5.3 μm [4] and the InSb focal plane arrays (FPAs) are an important component of the infrared thermal imager.

A standard optoelectronic system includes the photonics devices and the electronics devices. Most of electronic devices

Optoelectronic Devices and Integration VIII, edited by Xuping Zhang, Baojun Li, Changyuan Yu, Xinliang Zhang, Daoxin Dai, Proc. of SPIE Vol. 11184, 1118411
 · doi: 10.1117/12.2536915

are based on GaAs and Si, therefore, the integration of InSb photodetector on the a GaAs or Si wafer is a promising approach to further develop the performance, decrease the energy and expand the application of the InSb photodetectors. For example, the requirement of the next-generation MIR FPAs is the small pixel size and ultra-low energy cost [5]. The InSb on GaAs or Si wafer can realize the InSb detectors and GaAs or Si-based read-out circuits operate in a single wafer and avoid the additional room and energy cost of the connecting component. Moreover, the integration of InSb detectors on Si is essential for the MIR Si photonics. Compared with the recent Si photonics operating in the near-infrared region, the operated wavelength MIR Si photonics extends the operated wavelength to MIR region which is a fundamental technique to realize the on-chip bio-/chemo-sensors, the on-chip/intra-chip MIR communication, and the wearable devices operated at the MIR region [6, 7].

Heteroepitaxial growth of InSb on Si wafers is a simple method to monolithically integrate InSb on Si which can realized a large-sized InSb on Si wafer and doesn't require a complicated wafer bonding process and isn't restricted by the size of the InSb wafer. High lattice constant is the main challenge for the growth of InSb on GaAs and Si where the lattice mismatch between InSb/GaAs is 14.6% and that between InSb/Si is up to 19.3%. The dislocations associated with the lattice mismatch seriously increase the dark current of photodetector, Huffaker *et al.* proposed a novel growth method, known as interfacial misfit (IMF) array, to grow III-V compound semiconductors on mismatch substrates, such as GaSb/GaAs [8], InSb/GaAs [9], and AlSb/Si [10]. Under carefully controlled growth conditions, uniform misfit dislocation are formed at the interfacial to relieve the strain energy associated with the lattice mismatch in the heretoepitaxy. For the growth of InSb/Si, two extra challenges exist: 1) different crystal structures where InSb is the zinc-blend structure and Si is the diamond-like structure, which results in the anti-phase domain; 2) InSb layer can't form on the surface of (100) Si due to the Sb atoms prefer to bond with the Si atoms rather than In atoms [11]. Therefore, a buffer layer is require in the growth of InSb on Si. Previous research suggested an antimonide buffer layer, including AlSb, GaSb and InSb quantum dots could effectively improve the material quality of InSb layers on Si where a 300 K electron mobility of 20,202 $cm^2/V{\cdot}s$ [12]. Therefore, the heteroepitaxy of the InSb photodetector on GaAs/Si is feasible. Besides improving the quality of InSb layer, inserting a wide bandgap semiconductor layer in the absorption region (i-layer) is another approach to decrease the dark current of the photodetector. Savich *et al.* proposed this architecture, named as unipolar barrier detector. In this architecture, only one kind of carrier (electron or hole) flow across the photodetector while the other kind of carrier is impeded [13]. Ultra-low dark current has been achieved via this architecture in the InAs and InAsSb infrared photodetectors [14, 15]. The InAs photodetector with a 100 nm $InAs_{0.18}Sb_{0.82}$ electron barrier owned a 77 K R_0A near "Rule-07" which assumes all dark current is Auger-limited [13, 16].

This study aimed to investigate the influence of an electron barrier in the InSb detector on its electrical and optical properties. Based on the bandgap diagram, the effect of the barrier on the dark current was discussed. The numerical simulation about the quantum efficiency of the photodetector with and with barrier was presented and discussed associated the heteroepitaxy.

2. METHODS

The simulation was based on the schematics of InSb PIN photodetector shown in Figure 1 where two same structures of the InSb photodetector are grown on a (100) Si substrate and a (100) GaAs substrate, respectively. For the sample on Si, an antimonide buffer is inserted between the photodetector and the Si substrate and its function and structure are demonstrated in the introduction. IMF arrays exist at both the buffer/Si and the InSb/buffer interfaces and their

microstructures were investigated in the previous research [12]. The structure of InSb PIN photodetector includes a 50 n+ InSb contact layer, InSb i-layer, a 25 nm $In_{0.9}Al_{0.1}Sb$ barrier inserting in the i-layer, a 50 nm p InSb layer and a 200 nm p+ contact layer. The lattice constant of $In_{0.9}Al_{0.1}Sb$ is about 6.35 Å which is slightly smaller than that of InSb (6.479 Å), therefore, the thickness of the barrier is limited because a high thickness may result in extra defects in strain layer. The i-layer is unintentionally n-type doped which is common in the heteroepitaxy of InSb by molecular beam epitaxy [17].

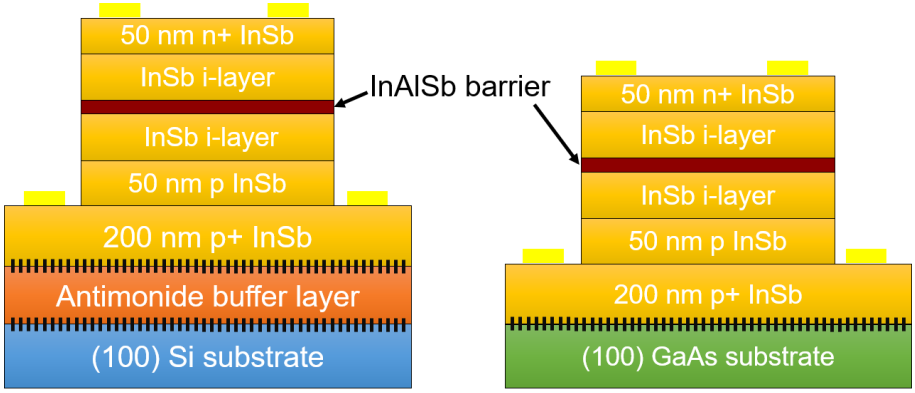

Figure 1 Schematics of InSb PIN photodetector on (100) Si and (100) GaAs substrates. A series of black lines at the interfaces indicate the interfacial misfit dislocations.

The numerical simulation of the photodetector is based on the one-dimensional steady-state continuity equation [18, 19]. The wavelength of incident light is 5.3 μm, the bias voltage is (photovoltaic mode) and the temperature is 77 K. The electron barrier layer is assumed to be ideal which totally imped the transportation of electrons. The hole transportation in the n-type semiconductor is described using $D_p\left(\frac{d^2p_n}{dx^2}\right) + G(5.3, x)$- $\frac{p_n - p_{n0}}{\tau_p}$=0, where G(5.3, x) is the generation rate of electron-hole pairs under the incident light of 5.3 μm and its value is described using $G(\lambda, x) = \alpha(\lambda)\phi(\lambda)[1 - R(\lambda)]\exp[-\alpha(\lambda)x]$. $\alpha(\lambda)$ is the wavelength dependent absorption coefficient which is 3100 cm^{-1} at 5.3 μm. $R(\lambda)$ is the wavelength dependent reflectivity which is 0.65 at 5.3 μm. q is the elementary charge; and p_n, p_{n0}, τ_p, and D_p are the hole density, the intrinsic hole density, the hole lifetime, and the hole diffusion coefficient, respectively, in the n-type InSb. τ_p and D_p can be instead by the diffusion length of the hole (L_p) which is express as $L_p = \sqrt{D_p \times \tau_p}$. The value of L_p can be experimentally measured. For the bulk n-type InSb, Lp is about 32-38 μm [20] and the L_p of the InSb layer on a mismatch substrate is about 5-10 μm. The contribution of the 50 nm n+ contact layer to the photoresponse isn't considered because the contact layer is heavily doped and its absorption edge is shifted to 4 μm due to the Moss-Burstein effect [18]. The contribution of the 50 nm p layer is also not considered due to its small thickness and bottom position. Other absorption mechanisms (free carrier, defect, and exciton) are not considered in this simulation. The hole current density is given by $J_p = qD_p(\frac{dp}{dx}\Big|_{x=L})$, where L is the length of the absorption region. In this simulation, the absorption region depends on the architecture of the photodetector. Finally, The quantum efficiency is calculated using $\mathrm{QE} = \frac{J_p}{q\phi}$.

3. RESULTS AND DISCUSSION

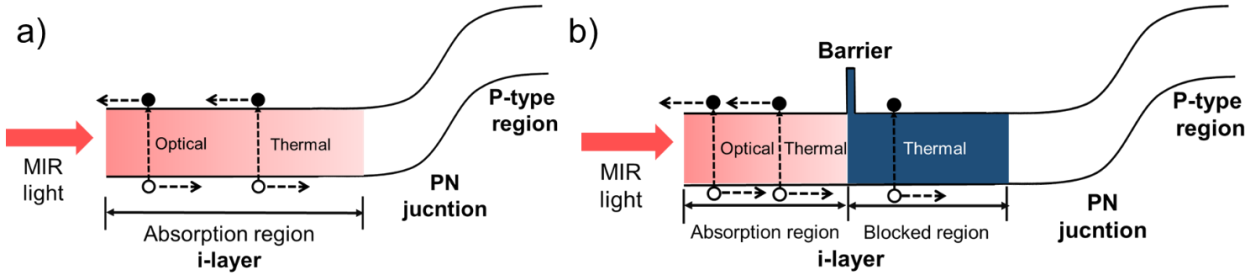

Figure 2 Bandgap diagrams of (a) the standard InSb PIN photodetector and (b) the InSb PIN photodetector with a barrier. The n+ and p+ contact layers are not shown. The red parts of the i-layers contribute to the quantum efficiency of the photodetector in the simulation, while, the blue part of the i-layer does not.

The bandgap diagram of a standard InSb PIN photodetector is shown in Figure 2(a). As mentioned above, only the i-layer is consider as the absorption region. The incident light is absorb in this region and excites electron-hole pairs, named as photo-generated carriers, which are collected by contacts. Meanwhile, other factors also excite electron-hole pairs to form dark current. Generally, factors include the diffusion current caused by thermal excitation, the generation-recombination current, the tunneling current and surface leakage. Although it's very difficult to obtain the value of the dark current, it can be disused based on the bandgap diagrams. For the narrow bandgap material-based photodetector, the diffusion current caused by thermal excitation is the main reason for the dark current due to its small bandgap. For the InSb layer on a mismatch substrate, its defect density is high, therefore, the generation-recombination, and tunneling current is also remarkable. Most of these two kinds of dark current generate at the PN junction [21, 22]. The surface leakage is mainly related to the surface defects which can be suppress via surface passivation [23].

Figure 2(b) shows the bandgap diagram of the photodetector with an electron barrier and the bandgap of $In_{0.9}Al_{0.1}Sb$ is 0.54 eV at 77 K. Assuming the barrier is ideal, i.e., no electron is allowed to transport across it. The barrier divides the i-layer into two parts. The properties red part at its left is similar to the i-layer shown in Figure 2(a) where both photo-generated and thermal excited carriers can be collected by contacts. The electron generating in the blue region can't be collected by the n+ contact due to the barrier, therefore, this region makes no contribution the photoresponse. In this simulation, the red region is named as the absorption region, while, the blue region is named as the blocked region. Although the existence of the barrier impedes the transportation of the photo-generated electrons in the i-layer, it also impede the dark current generating in the PN junction and the blocked region. The ideal barrier can totally suppress the generation-recombination and tunneling current. The thermal excited dark current in the blocked region is also suppressed by the barrier.

The influence of InAlSb barrier layer on the quantum efficiency (QE) of the InSb photodetector are simulated under different device parameters (the diffusion length of hole, the thickness of absorption region and blocked region). The length of the blocked region is 1 μm except for the case shown in Figure 3(d). The simulated QE of the photodetector without the barrier is firstly shown in Figure 3(a). QE increases to a peak when the length of the absorption region increases. The position of the QE peaks vary with the different diffusion length of hole (L_p) and the peak positions shift to right, i.e., the higher absorption region thickness ($L_{absorption}$) with an increasing L_p. When $L_{absorption}$ is below 2 μm, the L_p doesn't influence the QE. When $L_{absorption}$ exceeds 2 μm, the QE strongly depends on the L_p and a higher L_p results in a higher QE when $L_{absorption}$ is fixed. Therefore, the $L_{absorption}$ should be above 2 μm to avoid the QE limited by the

insufficient $L_{absorption}$ and increasing L_p is another approach to increase QE when the $L_{absorption}$ is above 2 μm. Figure 2(b) shows the simulated QE for the photodetector with the barrier. The existence of the InAlSb barrier doesn't change the shapes of curves where all QE increases to peaks and then decrease with an increasing $L_{absorption}$.

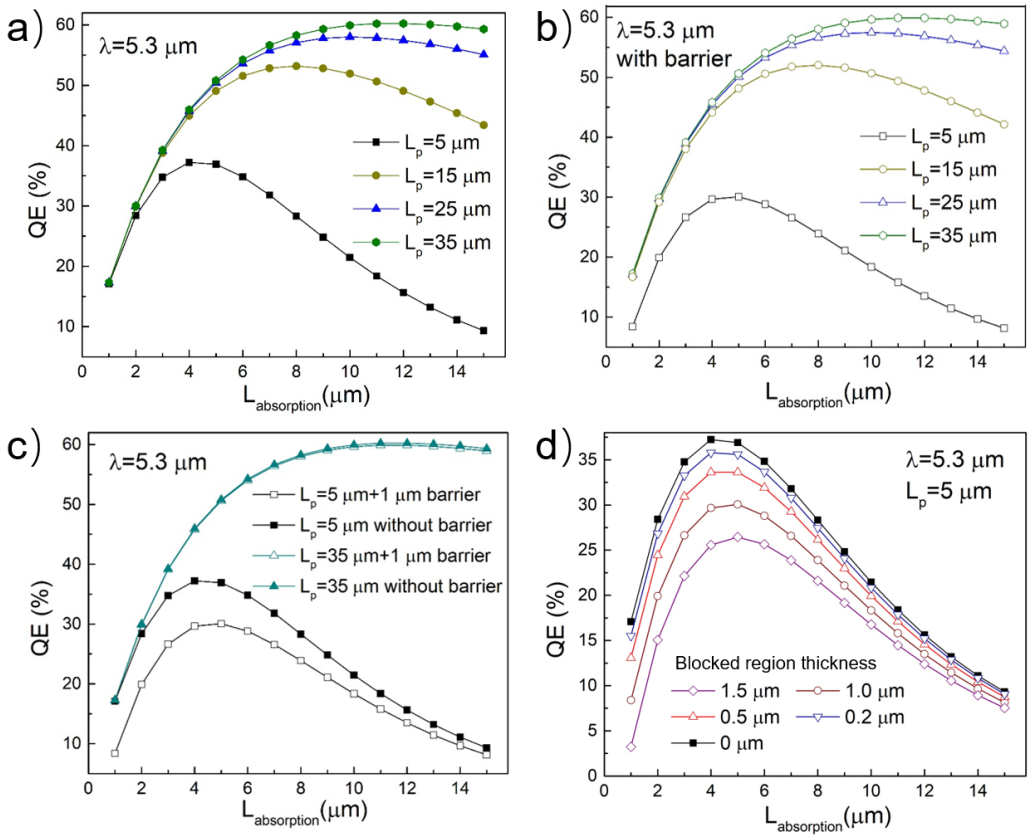

Figure 3 The simulated quantum efficiency (QE) of the InSb PIN photodetectors with/without the barrier as a function of the absorption region thickness ($L_{absorption}$) when the wavelength of incident light is 5.3 μm. a) QE depends on the diffusion length (L_p) for the detector without the barrier. b) QE depends on the diffusion length for the detector with the barrier. c) Comparison of QE for the detectors with/without the barrier when the diffusion lengths are 5 μm and 35 μm. d) QE depends on the blocked region thickness.

The comparison between the simulated QE of the photodetector with and without the barrier is shown in Figure 3(c) where the solid squares indicate the QE of the photodetector without the barrier and the hollow squares indicate that of the photodetector with the barrier. For the case of L_p=5 μm, the barrier decrease the QE and its effect is more remarkable when $L_{absorption}$ is below 10 μm. For example, the QE is 37.2% for the photodetector without the barrier, while, the QE decreases to 29.7% for the photodetector with the barrier when the $L_{absorption}$=4 μm. In the heteroepitaxy, the thickness of epilayer is always restricted below 5 μm to avoid cracking caused by thermal mismatch [24], therefore, the existence of the barrier suppresses the QE of the InSb photodetector on a mismatch substrate when L_p is low. For the case of L_p=35 μm, the effect of the barrier on the QE is not remarkable because the L_p is much longer than the length of the blocked region (1 μm). The influence of the length of the blocked region was illustrated in Figure 4(d) when the L_p is 5 μm. Compared with the standard PIN photodetector (block region thickness is 0 μm), the photodetector with the barrier

exhibits a lower QE and the QE decreases with an increasing length of the blocked region. For the photodetector with a barrier, photo-generated electrons have to transport across the blocked region to reach the P-type region. Due to the limited L_p, parts of holes recombine in the transportation which result in a lower QE and the rate of the electrons that have been recombined increases with an increasing length of the blocked region. The simulation suggested the insufficient length of the absorption layer, the inappropriate position of barrier layer and the low diffusion length of hole are all reasons of the low QE. The existence of the barrier suppresses the QE of the photodetector and its effect depends on both L_p and its location. For the InSb photodetector on a mismatched substrate, its L_p is low due to its high defect density, therefore, its QE is seriously suppressed. The optimization of the location of the barrier is very important for the photodetector with a low L_p and locating the barrier as close to the PN junction as possible can increase the QE, however, its possible effect on the PN junction requires further research. In addition, the photodetector with a high L_p is not sensitivity to the location barrier, therefore, a high quality can increase the free degree of designing an InSb photodetector.

4. CONCLUSION

The existence of $In_{0.9}Al_{0.1}Sb$ electron barrier layer can effectively decrease the dark current of the InSb photodetector. An ideal barrier can totally the dark current caused by generation-recombination current, tunneling current and partially suppress the diffusion current. The simulation suggests a sufficient length of absorption region is important for a high QE. The effect of the barrier on the diffusion current depends on the location of the barrier. For the photoresponse, the barrier suppresses the QE and its effect depends on the diffusion length of hole and the location of the barrier. A high QE can be achieved via optimizing the architecture of the photodetector.

ACKNOWLEDGEMENTS

This work was supported by “the Fundamental Research Funds for the Central Universities (WUT: 193109004)” and National Innovation and Entrepreneurship Training Program for College Student (20191049709021). The authors of this paper would like to express their gratitude to Dr. Zheng Yi for his assistance with the valuable discussion.

REFERENCES

[1] A. Rogalski, “Infrared detectors: status and trends,” Progress in Quantum Electronics, 27(2-3), 59-210 (2003).

[2] J. Hodgkinson, and R. P. Tatam, “Optical gas sensing: a review,” Measurement Science and Technology, 24(1), 012004 (2012).

[3] M. Razeghi, “Overview of antimonide based III-V semiconductor epitaxial layers and their applications at the center for quantum devices,” European Physical Journal-Applied Physics, 23(3), 149-205 (2003).

[4] A. Rogalski, “Quantum well photoconductors in infrared detector technology,” Journal of Applied Physics, 93(8), 4355-4391 (2003).

[5] A. Rogalski, J. Antoszewski, and L. Faraone, “Third-generation infrared photodetector arrays,” Journal of Applied Physics, 105(9), (2009).

[6] G. Mashanovich, “Mid-Infrared Silicon Photonics,” Proceedings of SPIE - The International Society for Optical

Engineering, 8990, (2013).
[7] R. Soref, “Mid-infrared photonics in silicon and germanium,” Nature Photonics, 4(8), 495-497 (2010).
[8] S. H. Huang, G. Balakrishnan, M. Mehta *et al.*, “Epitaxial growth and formation of interfacial misfit array for tensile GaAs on GaSb,” Applied Physics Letters, 90(16), (2007).
[9] B. W. Jia, K. H. Tan, W. K. Loke *et al.*, “Effects of surface reconstruction on the epitaxial growth of III-Sb on GaAs using interfacial misfit array,” Applied Surface Science, 399, 220-228 (2017).
[10] S. Huang, G. Balakrishnan, A. Khoshakhlagh *et al.*, “Simultaneous interfacial misfit array formation and antiphase domain suppression on miscut silicon substrate,” Applied Physics Letters, 93(7), 071102 (2008).
[11] G. Franklin, D. Rich, H. Hong *et al.*, “Interface formation and growth of InSb on Si (100),” Physical Review B, 45(7), 3426 (1992).
[12] B. W. Jia, K. H. Tan, W. K. Loke *et al.*, “Growth and characterization of InSb on (100) Si for mid-infrared application,” Applied Surface Science, 440, 939-945 (2018).
[13] G. Savich, J. Pedrazzani, D. Sidor *et al.*, “Dark current filtering in unipolar barrier infrared detectors,” Applied Physics Letters, 99(12), 121112 (2011).
[14] S. Maimon, and G. Wicks, “n B n detector, an infrared detector with reduced dark current and higher operating temperature,” Applied Physics Letters, 89(15), 151109 (2006).
[15] P. Klipstein, "XBn’barrier photodetectors for high sensitivity and high operating temperature infrared sensors." 6940, 69402U.
[16] W. Tennant, ““Rule 07” revisited: Still a good heuristic predictor of p/n HgCdTe photodiode performance?,” Journal of Electronic Materials, 39(7), 1030-1035 (2010).
[17] M. Debnath, T. Zhang, C. Roberts *et al.*, “High-mobility InSb thin films on GaAs (001) substrate grown by the two-step growth process,” Journal of crystal growth, 267(1-2), 17-21 (2004).
[18] Z. Djuric, B. Livada, V. Jovic *et al.*, “Quantum efficiency and responsivity of InSb photodiodes utilizing the Moss-Burstein effect,” Infrared Physics, 29(1), 1-7 (1989).
[19] S. M. Sze, and K. K. Ng, [Physics of semiconductor devices] John wiley & sons, (2006).
[20] B.-L. Chen, Y. Zhang, X. Fang *et al.*, "Determination of hole diffusion length in n-InSb at 80 K." 4369, 436-441.
[21] C. Canedy, E. Aifer, J. Warner *et al.*, “Controlling dark current in type-II superlattice photodiodes,” Infrared Physics & Technology, 52(6), 326-334 (2009).
[22] J. Y. Wong, “Effect of trap tunneling on the performance of long-wavelength $Hg_{1-x}Cd_xTe$ photodiodes,” IEEE Transactions on Electron Devices, 27(1), 48-57 (1980).
[23] I. Bloom, and Y. Nemirovsky, “Surface passivation of backside-illuminated indium antimonide focal plane array,” IEEE transactions on electron devices, 40(2), 309-314 (1993).
[24] H. Kawanami, “Heteroepitaxial technologies of III–V on Si,” Solar energy materials and solar cells, 66(1-4), 479-486 (2001).